Available online at www.sciencedirect.com
ScienceDirect
Marine Chemistry 109 (2008) 307–317
MARINE CHEMISTRY
www.elsevier.com/locate/marchem

Radium tracing of submarine groundwater discharge (SGD) and associated nutrient fluxes in a highly-permeable bed coastal zone, Korea

Guebuem Kim *, Jae-Woong Ryu, Dong-Woon Hwang

School of Earth & Environmental Sciences/RIO, Seoul National University, Seoul 151-747, Korea

Received 1 March 2007; received in revised form 5 July 2007; accepted 9 July 2007
Available online 17 July 2007

Abstract

In order to estimate submarine groundwater discharge (SGD) and SGD-driven nutrient fluxes, we measured the concentrations of nutrients, ^{224}Ra, and ^{226}Ra in seawater, river water, and coastal groundwater of Yeongil Bay (in the southeastern coast of Korea) in August 2004 and February 2005. The bottom sediments over the shallow areas of this bay are composed mainly of coarse sands. Large excess concentrations of ^{224}Ra, ^{226}Ra, and Si supplied from SGD were observed in August 2004, while these excess concentrations were not apparent in February 2005. Based on the mass balance for ^{224}Ra, ^{226}Ra, and Si, which showed conservative mixing behavior in seawater, SGD was estimated to be approximately 6×10^6 m^3 day^{-1} (seepage rate = 0.2 m day^{-1}) in shallow areas (<9 m water depth) in August 2004, which is much higher than the SGD level typically found in other coastal regions worldwide. During the summer period, SGD-driven nutrients in this bay contributed approximately 98%, 12%, and 76% of the total inputs for dissolved inorganic nitrogen (DIN), phosphorus (DIP), and silicate (DSi), respectively. Our study implies that the ecosystem in this highly permeable bed coastal zone is influenced strongly by SGD during summer, while such influences are negligible in winter.

Keywords: Submarine springs; Groundwater pollution; Radium isotopes; Nutrients; Korea; Yeongil Bay

1. Introduction

Submarine discharge of fresh groundwater, re-circulating seawater, and their composites into the ocean has been recognized as an important pathway for transporting chemical constituents originating from the continents (Moore, 1996; Burnett et al., 2003; Kim et al., 2005). SGD occurs mainly in the form of nearshore seepage, offshore seepage, and submarine springs (Burnett et al., 2001; Taniguchi et al., 2002; Moore, 2003; Kim et al., 2003).

Among these forms, the discharge of coastal brackish groundwater by advective porewater flow may be volumetrically and ecologically more important than submarine springs, due to large seeping areas along almost the entire coastal zone and much higher concentrations of some chemical constituents (Li et al., 1999; Burnett et al., 2001; Taniguchi et al., 2002; Kim et al., 2005). Although submarine springs occurring in offshore areas are more difficult to measure, they are known to be a widespread feature in many coastal areas of the ocean (Kohout, 1966; Zektzer et al., 1973; Johannes, 1980; Burnett et al., 2001; Swarzenski et al., 2001; Elhatip, 2003). These springs are in general related to an extensive network of underground caves and channels (Carruthers et al., 2005). In addition,

* Corresponding author. Tel.: +82 2 880 7508; fax: +82 2 876 6508.
E-mail address: gkim@snu.ac.kr (G. Kim).

0304-4203/$ - see front matter © 2007 Elsevier B.V. All rights reserved.
doi:10.1016/j.marchem.2007.07.002

Shaban et al. (2005) reported a direct correlation between SGD and local fracture systems on the basis of thermal anomalies using remote sensing along the northwestern coast of Lebanon.

Several recent studies showed that the magnitude of SGD is controlled mainly by diurnal and spring-neap tidal fluctuations on the basis of continuous measurements of natural tracers (^{222}Rn and CH_4) and automated seepage meters (Kim and Hwang, 2002; Taniguchi, 2002). The magnitude of SGD also displays large seasonal changes (Kelly and Moran, 2002; Michael et al., 2005). Michael et al. (2005) found that seawater was drawn into aquifers as the freshwater-saltwater interface moved landward during winter, and discharged back into coastal waters as the interface moved seaward in summer at Waquoit Bay, Massachusetts, USA.

Thus, in this study, we aimed at investigating seasonal changes in submarine inputs of groundwater and nutrients into Yeongil Bay where fractured bed-rocks are well developed. The magnitude of SGD was determined using ^{224}Ra, ^{226}Ra, and Si tracers, which are powerful for tracing SGD over large space and time scales.

2. Study area and analytical methods

2.1. Study area

Yeongil Bay is a unique semi-enclosed environment in the eastern coast of Korea (Fig. 1). This bay is relatively broad and deep, with an area of ~120 km^2 and a mean depth of ~20 m. The shallow areas of this bay consist mainly of coarse sediments (sand and gravel), whereas the other areas consist mainly of fine sediments, such as silt and clay (Park and Song, 1972). The major strike-slip Hupo fault and reverse fault run parallel to the coastal line, across the center of this bay (Chough et al., 2000).

The maximum tidal range of this bay is less than 25 cm. The annual precipitation is about 112 cm, with most of the precipitation during the summer (from June to September). The amount of freshwater entering into the bay through surface runoff is approximately 1.6×10^6 m^3 day^{-1}. Hyeongsan River contributes to about 90% of the freshwater discharge among all streams and rivers in this bay (Lee et al., 2003; Yoon et al., 2003). The current of this bay in general shows an anti-clockwise circulation (Kim et al., 2001a).

2.2. Sampling and analytical method

Water samples were taken from Yeongil Bay, groundwater wells, and Hyeongsan River, for the analyses of nutrients, pigments, and Ra isotopes during August 10–12, 2004 and February 20–23, 2005. The river-water samples were collected at one station (St. 10) in August 2004 and at 8 stations (St. 5–12) in February 2005 in the Hyeongsan River estuary, and the seawater samples were collected at 17 stations. The river and seawater samples were collected from the surface layer (~1 m water depth) using a submersible pump with a flow rate of 15–20 L min^{-1} onboard a ship for both sampling periods. The coastal groundwater samples (St. 1–4) were obtained from coastal wells (<20 m depth) and boreholes (<1 m depth) using an electric pump in August 2004.

For ^{224}Ra and ^{226}Ra measurements, about 80 L of seawater ($n=17$) and river water ($n=6$) and about 40 L of coastal groundwater ($n=4$) samples were collected in polypropylene cubitainers. The samples were directly passed through an acrylic column (4.5 cm in diameter, 20 cm in length) filled with MnO_2-impregnated acrylic fiber (~60 g-wet) in the field (under a flow rate of 1.0 L min^{-1}). This flow rate allows the quantitative adsorption of Ra onto the MnO_2-fiber (Moore and Reid, 1973; Kim et al., 2001b). In the laboratory, after any sea salts on the MnO_2-fibers were washed off, the water content of the fibers was adjusted. The activity of ^{224}Ra on the MnO_2-fiber was measured using a delayed coincidence counter (DCC, RaDeCC) (Moore and Arnold, 1996). Although both ^{224}Ra and ^{223}Ra activities were counted using DCC, we could not obtain statistically meaningful counts for ^{223}Ra in this region (a larger sample volume is required). About 20 days after ^{224}Ra was determined, the activity of ^{228}Th was measured via ^{224}Ra using DCC. The measured activity of ^{228}Th was negligible compared with the activity of ^{224}Ra. The activity of ^{226}Ra was measured by counting alpha emission of the ^{222}Rn daughter, ^{218}Po, using a radon-in-air monitor, RAD7 (Kim et al., 2001b). Here, the detection efficiencies of the DCC for ^{224}Ra and the RAD7 for ^{226}Ra were measured using ^{228}Th/^{232}U and ^{226}Ra standards, respectively, for the same weight of MnO_2-fiber.

To measure the concentrations of photosynthetic pigments, about 1-L samples of seawater were filtered through a GF/F filter (47 mm in diameter) in the field, and then the filters were stored immediately in a deep freezer (−80 °C). The concentrations of photosynthetic pigments were determined using a modified version of the method reported by Wright et al. (1991). First, the frozen filter was cut into small slices and then ground in a motorized grinder for 30 s. The photosynthetic pigments were extracted from the ground filter by applying 100% acetone (5 mL) at −20 °C for 24 h in the dark. After sonification and centrifugation, the acetone extract (1 mL) was mixed with 0.3 mL deionized water.

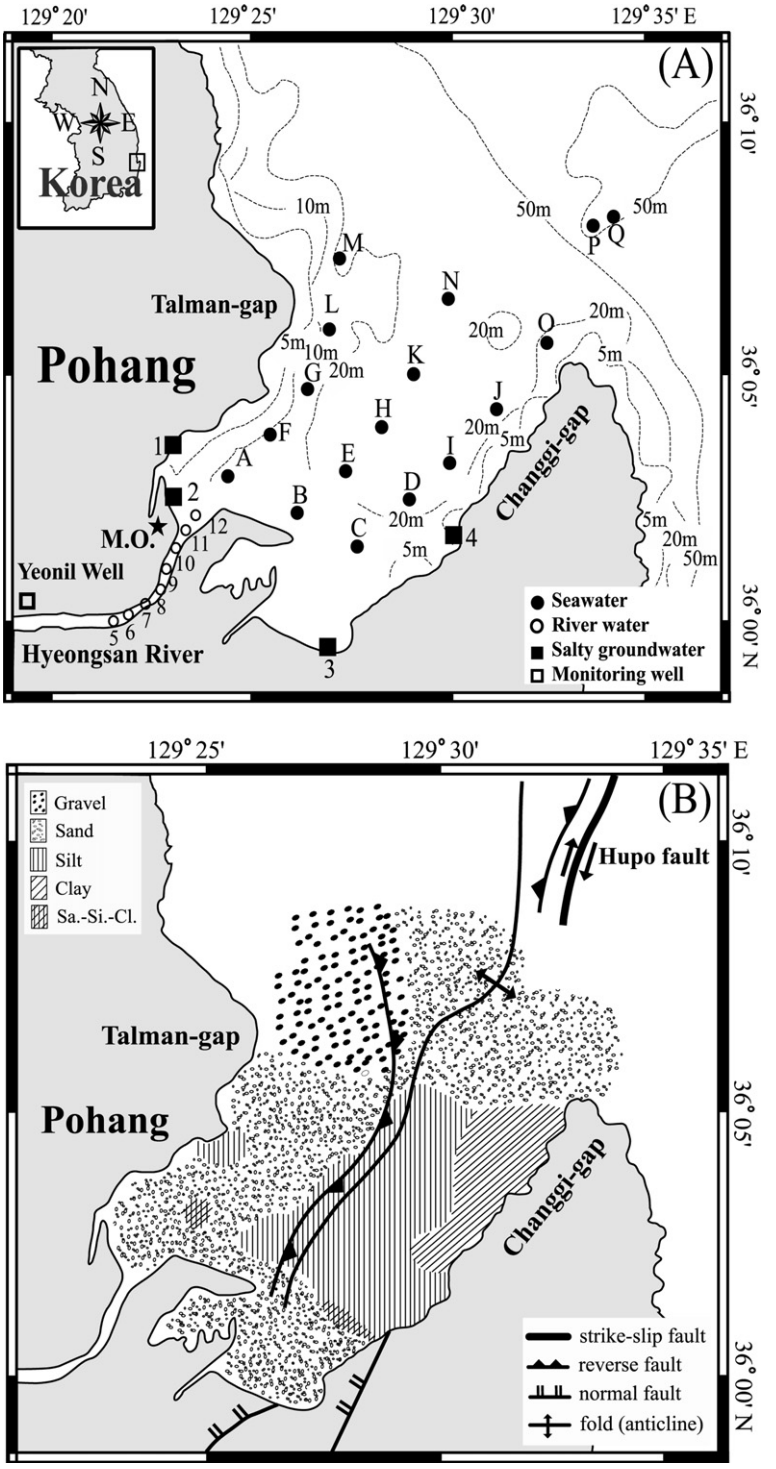

Fig. 1. A map showing the bathymetry and sampling sites (A) of Yeongil Bay in August 2004 and February 2005, and distribution of sedimentary facies (Park and Song, 1972) and geological structures (Chough et al., 2000) (B). The open square (A) represents the monitoring well for measuring the elevation of the water table. The filled star (A) represents the location for precipitation measurements.

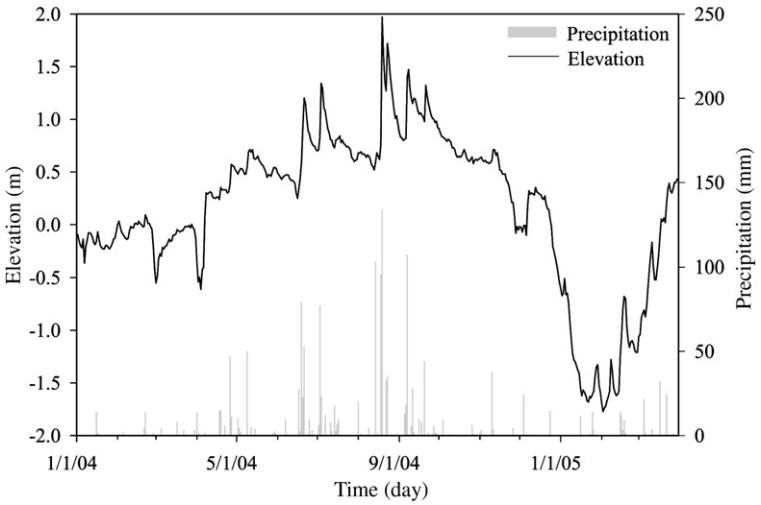

Fig. 2. Seasonal variations in precipitation and the elevation of the water table from January 2004 to March 2005.

The mixed solution (0.1 mL) was analyzed using a reverse-phase high performance liquid chromatography (Waters, Model 2695). The concentrations of photosynthetic pigments were calibrated using well-attested standards (Sigma Chemical and DHI).

Temperature and salinity were measured in situ using a portable salinometer (WTW, Model LF340) and CTD (SBE 25). Samples of nutrients (NO_3^-, NO_2^-, NH_4^+, PO_4^{3-}, and $Si(OH)_4$) were collected in polyethylene bottles and analyzed using an Auto-Analyzer (TRAACS 2000,

Table 1
Concentrations of nutrients and Ra isotopes in the surface seawater, river water, and coastal groundwater around Yeongil Bay during August 10–12, 2004

Station number	Location		Temperature (°C)	Salinity (ppt)	Nutrient concentration (μM)			Ra activity (dpm 100 L^{-1})	
	Latitude	Longitude			DIN	DIP	DSi	^{224}Ra	^{226}Ra
River water									
10	36°01′20″N	129°22′87″E	28.9	30.55	2.9	0.16	16	52±4	24±2
Groundwater									
1	36°03′08″N	129°22′47″E	22.0	5.9	126	0.75	73	281±7	56±7
2	36°02′04″N	129°22′52″E	23.6	18.8	245	0.21	133	570±9	72±7
3	35°59′19″N	129°27′14″E	28.6	20.6	235	0.21	95	155±4	36±4
4	36°01′18″N	129°30′16″E	26.6	7.8	634	0.43	43	103±7	32±4
Bay water									
A	36°02′74″N	129°24′49‴E	27.1	33.62	1.1	0.16	28	7.7±0.6	18.6±1.5
B	36°02′04″N	129°26′23″E	27.5	33.48	1.3	0.12	20	11.9±0.8	17.6±0.7
C	36°01′15″N	129°27′63″E	27.2	33.26	0.6	0.07	24	8.1±0.7	18.7±1.4
D	36°01′89″N	129°28′54″E	27.1	33.35	0.5	0.03	20	6.4±0.5	13.0±1.1
E	36°02′75″N	129°26′95″E	26.9	33.51	0.2	0.07	22	1.9±0.3	16.4±1.3
F	36°03′45″N	129°25′03″E	27.0	33.64	0.5	0.21	20	2.2±0.3	16.6±1.3
G	36°04′31″N	129°26′21″E	27.0	33.68	0.6	0.12	14	9.4±0.5	10.5±0.7
H	36°03′61″N	129°27′80″E	26.7	33.42	0.5	0.16	20	4.1±0.3	16.2±1.4
I	36°03′24″N	129°30′16″E	26.6	33.67	0.9	0.07	18	8.9±0.8	15.8±1.0
J	36°04′41″N	129°31′44″E	25.6	33.74	1.0	0.03	16	5.6±0.4	13.1±1.1
K	36°04′79″N	129°29′28″E	25.9	33.63	0.7	0.07	13	3.1±0.4	9.4±0.7
L	36°05′53″N	129°27′46″E	26.4	33.70	0.6	0.12	16	3.2±0.3	14.8±0.9
M	36°07′10″N	129°26′39″E	27.1	33.74	2.5	0.12	12	16.2±0.9	10.9±0.9
N	36°05′78″N	129°30′30″E	26.1	33.45	2.4	0.16	11	6.1±0.5	12.0±0.6
O	36°04′96″N	129°32′76″E	26.7	33.69	0.3	0.07	12	12.0±0.7	9.7±0.7
Offshore water									
P	36°06′53″N	129°33′37″E	25.5	33.72	0.4	0.12	9.1	4.8±0.4	11.3±0.7
Q	36°06′75″N	129°33′98″E	25.4	33.74	0.4	0.12	8.1	2.9±0.4	10.5±0.8

Bran+Lubbe K.K) in the laboratory. In this study, we define DIN as the sum of NO_3^-, NO_2^-, and NH_4^+, DIP as PO_4^{3-}, and DSi as $Si(OH)_4$. The content of suspended solids (SS) was determined by drying the suspended materials on a membrane filter (47 mm in diameter, 0.45 μm in pore size) at 110 °C for 1 h after rinsing with deionized water to remove sea salts.

3. Results and discussion

3.1. Seasonal changes in precipitation and water-table elevation

The record of precipitation at Songdo, Pohang (~0.5 km away from the southwestern part of Yeongil Bay) from January 2004 to March 2005 showed that most of the precipitation occurred during the wet seasons (from June to September 2004) (Fig. 2). In general, the time lag between changes in the amount of precipitation and groundwater recharge (or change of water table elevation relative to the mean sea level) is dependent on regional geological features, such as soil type, soil moisture, and topography. In the study region, most of the precipitation seems to filter rapidly into the ground, since the trend of seasonal variations in precipitation was similar to that of the water-table elevation in Yeonil well (~4 km away from the southwestern part of Yeongil Bay) over the same period (Fig. 2).

3.2. Spatial and seasonal changes in salinity, nutrients, and Ra isotopes in seawater

The salinity of surface seawater in the summer and winter periods ranged from 33.3 to 33.7 (mean=33.6, n=17) and from 33.5 to 34.5 (mean=34.0, n=17), respectively, with slightly lower values in the innermost area of the bay (Tables 1 and 2). The concentrations of DIN and DIP were relatively lower in the summer period than those in the winter period, while the concentrations of DSi were higher in the summer period than those in the winter period. The activities of ^{224}Ra and ^{226}Ra in surface seawater ranged from 1.9 to 16 dpm 100 L^{-1} and

Table 2
The content of suspended solids (SS) and nutrients, and the activity of Ra isotopes (^{224}Ra and ^{226}Ra) in the surface seawater and river water around Yeongil Bay during February 20–23, 2005

Station number	Location		Temperature (°C)	Salinity (ppt)	SS (mg L^{-1})	Nutrient concentration (μM)			Ra activity (dpm 100 L^{-1})	
	Latitude	Longitude				DIN	DIP	DSi	^{224}Ra	^{226}Ra
River water										
5	36°00′03″N	129°20′36″E	5.7	5.4	10.6	138	1.71	59	8.3±0.8	10±1
6	36°03′14″N	129°22′03″E	8.8	20.7	25.3	183	1.75	102	8.8±0.8	13±1
7	36°00′33″N	129°22′28″E	9.5	21.4	26.7	243	0.90	46	12.4±0.9	11±1
8	36°00′47″N	129°22′37″E	8.3	21.9	25.1	121	0.50	47	10.1±0.8	28±2
9	36°01′12″N	129°22′80″E	8.4	25.8	28.0	216	0.96	31	16.9±1.3	17±1
10	36°01′21″N	129°22′86″E	8.7	26.7	30.6	71	0.44	34	12.0±1.0	18±2
11	36°01′49″N	129°23′07″E	8.8	26.5	25.2	–	–	–	–	–
12	36°01′70″N	129°23′32″E	10.2	28.6	20.9	–	–	–	–	–
Bay water										
A	36°02′74″N	129°24′49″E	9.4	33.48	–	9.3	0.77	10.5	6.2±0.4	8.4±1.1
B	36°02′04″N	129°26′23″E	9.1	34.07	–	6.4	0.23	9.8	3.7±0.3	9.0±0.8
C	36°01′15″N	129°27′63″E	9.4	34.00	–	9.1	0.12	9.9	5.2±0.6	10.6±1.2
D	36°01′89″N	129°28′54″E	9.7	33.98	–	8.9	0.82	10.3	3.1±0.2	9.2±0.8
E	36°02′75″N	129°26′95″E	9.4	33.70	–	7.2	0.22	9.8	6.4±0.3	7.5±0.9
F	36°03′45″N	129°25′03″E	9.7	33.54	–	8.0	0.14	9.8	3.7±0.5	7.3±0.8
G	36°04′31″N	129°26′21″E	9.4	34.14	–	8.6	0.23	10.1	6.7±0.7	7.2±0.8
H	36°03′61″N	129°27′80″E	10.6	34.15	–	5.9	0.25	9.0	7.3±0.6	9.2±0.9
I	36°03′24″N	129°30′16″E	10.4	34.14	–	5.2	0.56	8.8	4.3±0.4	9.4±0.6
J	36°04′41″N	129°31′44″E	8.7	33.49	–	9.6	0.86	11.6	4.2±0.3	11.2±0.6
K	36°04′79″N	129°29′28″E	10.2	34.11	–	3.8	0.53	8.4	2.8±0.3	8.8±0.5
L	36°05′53″N	129°27′46″E	9.6	34.39	–	4.5	0.55	9.2	6.1±0.5	11.5±1.2
M	36°07′10″N	129°26′39″E	9.8	34.35	–	4.2	0.54	7.7	3.5±0.3	9.8±1.2
N	36°05′78″N	129°30′30″E	10.5	33.95	–	4.0	0.47	8.3	4.1±0.5	11.1±0.7
O	36°04′96″N	129°32′′76″E	10.4	33.96	–	3.7	0.49	8.1	2.6±0.4	8.0±0.6
Offshore water										
P	36°06′53″N	129°33′37″E	10.8	34.50	–	4.1	0.58	8.4	1.5±0.2	10.9±0.8
Q	36°06′75″N	129°33′98″E	10.2	34.49	–	5.4	0.30	8.6	1.3±0.2	10.9±0.8

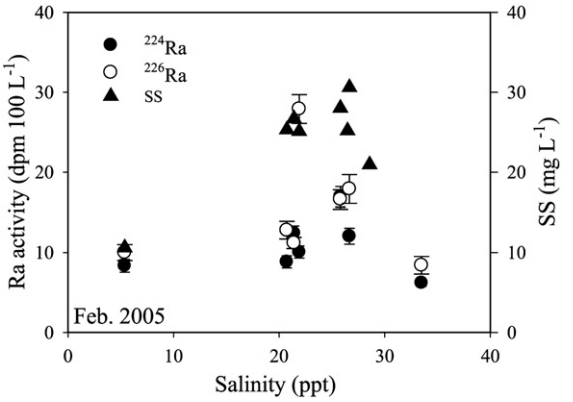

Fig. 3. Variations of ^{226}Ra, ^{224}Ra, and suspended solids (SS) with salinity in the Hyeongsan River estuary in February 2005.

9.4 to 19 dpm 100 L^{-1} in the summer period, respectively, and from 1.3 to 7.3 dpm 100 L^{-1} and 7.2 to 12 dpm 100 L^{-1} in the winter period, respectively. The concentrations of nutrients and Ra isotopes were highest in the innermost bay area in both sampling periods.

In the mixing zone of the Hyeongsan River estuary, the activities of the Ra isotopes, ^{224}Ra and ^{226}Ra, were much higher than those expected from the conservative mixing of river (lowest salinity) water and open ocean (highest salinity) seawater (Fig. 3). This indicates that excess Ra was supplied from other sources, such as desorption from riverine suspended particles, diffusion/advection from bottom sediments, and porewater/groundwater advection (Elsinger and Moore, 1984; Sarine et al., 1990; Yang et al., 2002). Based on this behavior of Ra in February 2005, we used the endmember salinity of river water higher than 26 for each season. This is to avoid the overestimation of excess Ra, which is used in the Ra budget model in the next section, due to Ra desorption from fresh suspended sediments inside the bay.

3.3. Estimating excess ^{226}Ra, ^{224}Ra, and DSi

The concentrations of ^{226}Ra, ^{224}Ra, and DSi in seawater during the summer period were higher than those during the winter period (Fig. 4). These higher concentrations in the summer period were much greater than those expected from the conservative mixing of river water and seawater end-members. The salinity of the river water endmember in summer was 30.55, which includes all Ra desorbed from fresh suspended matter from upstream based on Fig. 3. In contrast, the excess concentrations of ^{226}Ra and DSi were negligible in February 2005, although some excess activities of ^{224}Ra were observed. Negligible concentrations of excess ^{226}Ra and DSi during the winter period indicate a negligible level of SGD. Although the ingrowth of ^{226}Ra in sediments is negligible over a residence time scale of this bay, the half life of ^{224}Ra is short enough for ingrowth of the nuclide.

The excess concentrations for ^{224}Ra, ^{226}Ra, and DSi in August 2004 should be from other sources such as SGD, desorption from suspended particles and/or diffusion from bottom sediments. The concentrations of DSi and ^{226}Ra in seawater showed a clear positive correlation

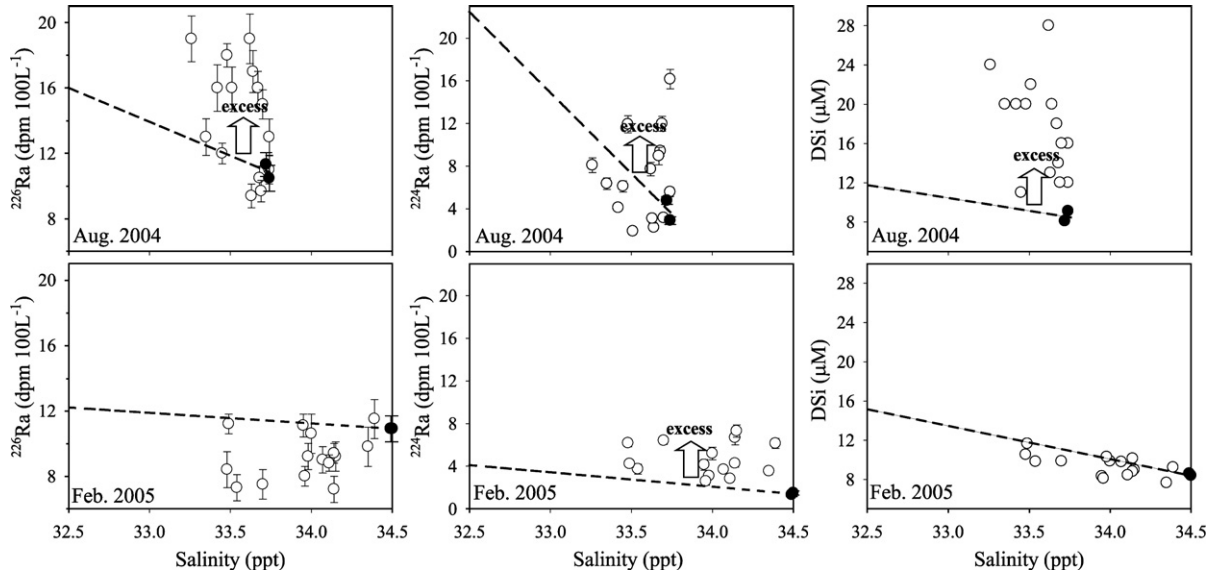

Fig. 4. Plots of salinity versus excess ^{226}Ra, ^{224}Ra, and DSi concentrations in surface seawater of Yeongil Bay in August 2004 and February 2005. The open and filled circles represent bay water and open ocean water, respectively. The dotted line represents the expected concentration due to conservative mixing between river water and open ocean water from outside the bay.

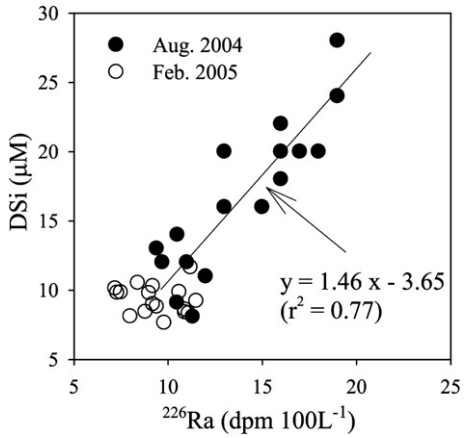

Fig. 5. A plot of ^{226}Ra activities versus DSi concentrations in the surface seawater of the study region in August 2004 and February 2005.

(r^2=0.77) during the summer period (Fig. 5). Thus, we used Si as a SGD tracer, together with ^{226}Ra and ^{224}Ra. Since the excess concentrations of these SGD tracers were negligible during the winter period, we calculated the SGD only for the summer period.

In order to calculate the excess Ra and DSi concentrations in seawater during the summer period, the chemical mass balance for ^{226}Ra, ^{224}Ra, and DSi can be expressed by the following equations:

$$^{226}\mathrm{Ra}_{\mathrm{Ex}} = {}^{226}\mathrm{Ra}_{\mathrm{B}} - f\,{}^{226}\mathrm{Ra}_{\mathrm{O}} - (1-f)\,{}^{226}\mathrm{Ra}_{\mathrm{E}} \quad (1)$$

$$^{224}\mathrm{Ra}_{\mathrm{Ex}} = {}^{224}\mathrm{Ra}_{\mathrm{B}} - f\,{}^{224}\mathrm{Ra}_{\mathrm{O}} - (1-f)\,{}^{224}\mathrm{Ra}_{\mathrm{E}} \quad (2)$$

$$\mathrm{DSi}_{\mathrm{Ex}} = \mathrm{DSi}_{\mathrm{B}} - f\mathrm{DSi}_{\mathrm{O}} - (1-f)\mathrm{DSi}_{\mathrm{E}} \quad (3)$$

where Ra_B and DSi_B, Ra_O and DSi_O, and Ra_E and DSi_E are the Ra and DSi concentrations in bay seawater, open ocean water, and estuarine end-members, respectively. Ra_{Ex} and DSi_{Ex} are the excess concentrations of Ra and DSi, respectively, and f is the fraction of the open ocean water. Here, f is calculated from the salinity of the measured values versus the salinity of open ocean water. The data at station 10 were used for the end-member values of the estuarine water, and those from stations P and Q (outside the bay) were used for the seawater end-member values. Based on these end-member values and the equations above (Eqs. 1–3), the excess concentrations of ^{226}Ra, ^{224}Ra, and DSi in bay seawater were calculated to be about 4.1 dpm 100 L^{-1}, 5.4 dpm 100 L^{-1}, and 8.8 μmol L^{-1}, respectively. Therefore, we estimate the magnitude of SGD in the next section using mass balance models for excess chemical tracers.

3.4. Estimating SGD using mass balance models for excess ^{226}Ra, ^{224}Ra, and DSi

The vertical temperature profiles showed a strong stratification at about 9 m depth during the summer period. Since most SGD generally takes place in shallow water depths (<3 m) (Taniguchi et al., 2002), the coastal brackish groundwater discharge influences mostly the surface layer (<9 m water depth). Thus, we confine the box model for excess Ra and DSi to only the upper 9 m.

In order to construct mass balance models for excess ^{226}Ra, ^{224}Ra, and DSi in surface waters, we have to account for all sources and sinks of each chemical species. The changes in the concentrations of excess ^{226}Ra, ^{224}Ra, and DSi in the surface layer may be expressed in the following simultaneous equations (Eqs. 4–6):

$$\frac{d^{226}\mathrm{Ra}_{\mathrm{Ex}}}{dt} = F_{\mathrm{Diff}}^{\mathrm{Ra-226}} + \left[C_{\mathrm{GW}}^{\mathrm{Ra-226}} \times A_{\mathrm{Bott}} \times \psi_{\mathrm{SGD}}\right] - \left[C_{\mathrm{ex}}^{\mathrm{Ra-226}} \times V_{\mathrm{S}}(\lambda_{\mathrm{Ra-226}} + \lambda_{\mathrm{Mix}})\right] \quad (4)$$

$$\frac{d^{224}\mathrm{Ra}_{\mathrm{Ex}}}{dt} = F_{\mathrm{Diff}}^{\mathrm{Ra-224}} + \left[C_{\mathrm{GW}}^{\mathrm{Ra-224}} \times A_{\mathrm{Bott}} \times \psi_{\mathrm{SGD}}\right] - \left[C_{\mathrm{ex}}^{\mathrm{Ra-224}} \times V_{\mathrm{S}}(\lambda_{\mathrm{Ra-224}} + \lambda_{\mathrm{Mix}})\right] \quad (5)$$

$$\frac{d\mathrm{Si}_{\mathrm{Ex}}}{dt} = F_{\mathrm{Diff}}^{\mathrm{Si}} + \left[C_{\mathrm{GW}}^{\mathrm{Si}} \times A_{\mathrm{Bott}} \times \psi_{\mathrm{SGD}}\right] - \left[C_{\mathrm{ex}}^{\mathrm{Si}} \times V_{\mathrm{S}} \times \lambda_{\mathrm{Mix}}\right] \quad (6)$$

where the terms on the right side of the equations represent input fluxes through diffusion from bottom sediments (the first term), submarine groundwater flow (the second term), and output fluxes through radioactive decay and mixing with open ocean water (the final term). The definitions and values of each term are shown in Table 3.

The ingrowth for ^{224}Ra and ^{226}Ra in surface seawater was neglected since the activities of ^{228}Th and ^{230}Th in surface seawater were relatively negligible. At steady state, we can determine the two unknown terms, the seepage rate of groundwater (Ψ_{SGD}) and residence time of bay water ($1/\lambda_{\mathrm{Mix}}$), by using any pair of three simultaneous equations (Eqs. 1 and 2, Eqs. 1 and 3, Eqs. 2 and 3). Although this mass-balance approach was attempted for the first time by Hwang et al. (2005a) using ^{223}Ra, ^{226}Ra, and Si, there was an error for the decay constant of ^{223}Ra. This error was later corrected in Hwang et al. (2005b). In this study, we do not include ^{223}Ra due to large counting errors, but ^{224}Ra is included although uncertainties for the diffusion from bottom sediments and radioactive decay are larger. Our recent experience using this mass-balance approach showed that it is quite accurate for

Table 3
The definition and values used in the simultaneous equations for ^{226}Ra, ^{224}Ra, and DSi mass balances for calculating the residence time of bay water and the seepage rates of coastal groundwater in Yeongil Bay, Korea

	Definition	Value			Unit
		^{226}Ra	^{224}Ra	DSi	
F_{Diff}	Diffusive flux from bottom sediment ($R_G \times A_{Bott}$) for ^{226}Ra, ^{224}Ra, and DSi	1.3×10^{6}	6.3×10^{8}	1.5×10^{8}	dpm (or mmol) day^{-1}
	R_G : regeneration rate of ^{226}Ra, ^{224}Ra, and Si	0.044	21	5	dpm (or mmol) m^{-2} day^{-1}
C_{GW}	Concentration in groundwater for ^{226}Ra, ^{224}Ra, and Si	490	2773	86	dpm (or mmol) m^{-3}
A_{Bott}	Bottom area of bay (water depth: <9 m)	3.0×10^{7}	3.0×10^{7}	3.0×10^{7}	m^2
Ψ_{SGD}	Seepage rate of submarine groundwater	?	?	?	m day^{-1}
C_{ex}	Excess concentration in bay water for ^{226}Ra, ^{224}Ra, and DSi	41	54	8.8	dpm (or mmol) m^{-3}
V_S	Water volume of bay	1.0×10^{9}	1.1×10^{9}	1.1×10^{9}	m^3
λ_{Ra}	Decay constant: λ_{Ra-226} and λ_{Ra-224}	1.2×10^{-6}	0.19	–	day^{-1}
λ_{Mix}	Exchange rate between bay water and open-ocean water	?	?	?	day^{-1}

gauging high SGD rates (similar to those in this study region). However, larger differences in SGD often resulted for different tracer pairs from the same region, perhaps due to a large natural variability in groundwater endmembers.

Here, we estimated the corresponding diffusive fluxes from bottom sediments on the basis of the area of bay water (shallower than 9 m) multiplied by the assumed diffusive fluxes of ^{226}Ra, ^{224}Ra, and DSi from the coastal sediments reported by Charette et al. (2001), Bird et al. (1999), and Jung and Cho (2003), respectively. Although there are large uncertainties in these estimations, the errors of calculated SGD caused by this assumption appear to be relatively small. The diffusive fluxes of ^{224}Ra from bottom sediments are known to be similar for different sedimentary facies (Bird et al., 1999). The diffusive fluxes for the long-lived ^{226}Ra appear to be negligible over this time scale (~days).

The end-member concentrations of ^{226}Ra, ^{224}Ra, and DSi in coastal groundwater were determined from the average concentrations of four brackish groundwater samples (490±186 dpm m^{-3} for ^{226}Ra, 2773 ±2090 dpm m^{-3} for ^{224}Ra, and 86±38 mmol m^{-3} for DSi) due to the limitation of available "brackish" wells around this bay. Since these tracers are more highly enriched in brackish groundwater relative to fresh groundwater, we only include the "brackish" groundwater endmember in order to avoid an overestimation of SGD. Although there are large uncertainties in the quantification of SGD using this limited number of brackish groundwater samples, the range of endmember values falls into that of brackish groundwater generally found along the Korean Peninsula coasts (Hwang et al., 2005a; Kim et al., 2005). Since the main conclusion of this study is about the large difference in SGD between winter and summer in this highly permeable geological conditions, our results seem to be qualitatively more important.

The residence times of bay water ($1/\lambda_{Mix}$) were determined to be approximately 18, 12, and 16 days for the ^{226}Ra and ^{224}Ra pair, ^{226}Ra and DSi pair, and ^{224}Ra and DSi pair, respectively. The seepage rates (Ψ_{SGD}) were about 0.16, 0.26, and 0.17 m day^{-1} (mean=0.20 m day^{-1}) for the ^{226}Ra and ^{224}Ra pair, ^{226}Ra and DSi pair, and ^{224}Ra and DSi pair, respectively. Based on the bottom area of the shallow water (<9 m depth) and the estimated seepage rate, the discharge rates of submarine groundwater for the three tracer pairs were estimated to be approximately 4.9×10^{6}, 7.8×10^{6}, and 5.1×10^{6} m^3 day^{-1}, for which the mean (~6×10^{6} m^3 day^{-1}) is an order of magnitude higher than the river discharge (~6×10^{5} m^3 day^{-1}) during the summer period. These estimates may include the uncertainties caused by chemical analysis and the determination of end-member concentrations.

Although the magnitude of average seepage rates estimated in this study is slightly lower than that through the highly permeable volcanic rocks of Jeju Island, Korea (Kim et al., 2003), it is much higher than that through typical continental margins (Bugna et al., 1996; Cable et al., 1996; Corbett et al., 1999; Charette et al., 2001; Kelly and Moran, 2002). This large submarine discharge of groundwater (mostly brackish groundwater) in the shallow zone appears to be associated with the distribution of very coarse sandy sediments and a specific geological setting of bed-rocks.

3.5. Nutrient inputs through SGD and seasonal changes in pigments in seawater

The inputs of nutrients through SGD were calculated by multiplying the average concentrations of nutrients in coastal brackish groundwater (310±223,

0.40±0.26, and 86±38 μmol L^{-1} for DIN, DIP, and DSi, respectively) by the estimated average of SGD (6×10^6 m^3 day^{-1}). Since only four brackish groundwater samples were averaged for the calculation, this estimate includes large uncertainties. Nevertheless, we believe that this estimate is meaningful to compare the magnitude of nutrients through SGD with other sources in this bay. The results were approximately 190×10^4, 0.24×10^4, and 52×10^4 mol day^{-1} for DIN, DIP, and DSi, respectively, in the summer sampling period. Here, the loss of DIN by denitrification during the transport of groundwater within coastal sediment was neglected.

For comparison, the nutrient inputs through river water were determined by multiplying the discharge of river water ($\sim6\times10^5$ m^3 day^{-1}) by the concentrations of nutrients in river water (2.9, 0.16, and 16 μmol L^{-1} for DIN, DIP, and DSi, respectively). The input fluxes calculated from these assumptions were about 0.2×10^4, 0.01×10^4, and 1.0×10^4 mol day^{-1} for DIN, DIP, and DSi, respectively. The maximum nutrient inputs by diffusion from bottom sediments were also calculated by multiplying the bottom area of the bay ($\sim3\times10^7$ m^2) in the shallow depth (<9 m) by the regeneration rates of nutrients reported by Kim and Park (1998) and Jung and Cho (2003) (1.3, 0.6, and 5.0 mmol m^{-2} day^{-1} for DIN, DIP, and DSi from muddy sediments, respectively). The inputs of DIN, DIP, and DSi by diffusion from bottom sediments were estimated to be approximately 3.9×10^4, 1.8×10^4, and 15×10^4 mol day^{-1}, respectively. Here, the inputs of DIN, DIP, and DSi from the atmospheric deposition were not considered because they are generally very small relative to those from other sources in coastal areas off the Korean Peninsula (Yang, 2003). The nutrient inputs through SGD contribute at least 98%, 12%, and 76% of the total inputs for DIN, DIP, and DSi, respectively, in the summer period (Table 4). Thus, SGD appears to be the dominant source of DIN and DSi in this bay. Although there may be large uncertainties in this estimate, it is distinct in this study that there are large seasonal differences in SGD-driven nutrient fluxes, especially for DIN and DSi.

The concentrations of Chl. *a* and Chl. *b* in August 2004 ranged from 36 to1430 ng L^{-1} (mean=360 ng L^{-1}, n=15) and from 9 to 142 ng L^{-1} (mean=25 ng L^{-1}, n=15), respectively, in surface seawater during the summer period. During the winter period, those concentrations ranged from 199 to 735 ng L^{-1} (mean=468 ng L^{-1}, n=15) and 51 to 193 ng L^{-1} (mean=149 ng L^{-1}, n=15), respectively. In general, the concentrations were higher in the inner areas of the bay during the summer period, while they were higher over all stations during the winter period.

Table 4
A comparison of nutrient fluxes through river water, bottom sediments, and submarine groundwater discharge in Yeongil Bay

Pathway	Nutrient flux ($\times10^4$ mol day^{-1})		
	DIN	DIP	DSi
Hyeongsan river[a]	0.2	0.01	1.0
Diffusion from bottom sediments[b]	3.9	1.8	15
Submarine groundwater discharge[c]	190	0.24	52

[a]Based on the river discharge multiplied by the concentrations of nutrients in the Hyeongsan River.
[b]Calculated by multiplying the area by the regeneration rates of nutrients measured by Kim and Park (1998) and Jung and Cho (2003) in coastal bays and estuaries of Korea.
[c]Based on the average concentrations of nutrients in potential groundwater multiplied by the estimated SGD.

Considering the nutrient budgets, these distributions of pigments suggest that the higher concentrations in the innermost area in the summer period were associated mainly with the SGD-related DIN inputs. The overall higher pigment concentrations in the winter period were more likely influenced by strong vertical mixing of bottom waters highly enriched with nutrients, since the SGD inputs were negligible.

4. Conclusions

On the basis of ^{224}Ra, ^{226}Ra, and Si tracers, we found that SGD and associated nutrient fluxes in summer are much higher relative to other sources such as rivers and sedimentary diffusion, while they are almost negligible in winter, in Yeongil Bay. This implies that the fluxes of nutrients and other chemical constituents almost entirely depend on climatic conditions in highly permeable bed coastal zones. Thus, we suggest that a long-term monitoring strategy is necessary for evaluating SGD and environmental and ecological consequences of SGD in the coastal environment. We have to do more extensive future studies using tracers such as ^{15}N in order to determine the main source of excess nutrients occurring in brackish groundwater in this study region.

Acknowledgements

We thank Y.W. Lee and D.J. Joung who helped with sampling and pigment analyses. This work was supported by a research grant from the Korea Science and Engineering Foundation (KOSEF, R01-2006-000-10646-0). The manuscript was improved by comments from two anonymous reviewers and the guest editor, M. Charette (WHOI).

References

Bird, F.L., Ford, P.W., Hancock, G.J., 1999. Effect of burrowing macrobenthos on the flux of dissolved substances across the water-sediment interface. Marine Freshwater Research 50, 523–532.

Bugna, G.C., Chanton, J.P., Cable, J.E., Burnett, W.C., Cable, P.H., 1996. The importance of groundwater discharge to the methane budgets of nearshore and continental shelf waters of the northeastern Gulf of Mexico. Geochimica et Cosmochimica Acta 60, 4735–4746.

Burnett, W.C., Taniguchi, M., Oberdorfer, J., 2001. Measurement and significance of the direct discharge of groundwater into the coastal zone. Journal of Sea Research 46, 109–116.

Burnett, W.C., Bokuniewicz, H., Huettel, M., Moore, W.S., Taniguchi, M., 2003. Groundwater and pore water inputs to the coastal zone. Biogeochemistry 66, 3–33.

Cable, J.E., Bugna, G.C., Burnett, W.C., Chanton, J.P., 1996. Application of ^{222}Rn and CH_4 for assessment of groundwater discharge to the coastal ocean. Limnology and Oceanography 41, 1347–1353.

Carruthers, T.J.B., Tussenbroek, B.I., Dennison, W.C., 2005. Influence of submarine springs and wastewater on nutrient dynamics of Caribbean seagrass meadows. Estuarine, Coastal and Shelf Science 64, 191–199.

Charette, M.A., Buesseler, K.O., Andrews, J.E., 2001. Utility of radium isotopes for evaluating the input and transport of groundwater-derived nitrogen to a Cape Cod estuary. Limnology and Oceanography 46, 456–470.

Chough, S.K., Kwon, S.T., Ree, J.H., Choi, D.K., 2000. Tectonic and sedimentary evolution of the Korean peninsula: a review and new view. Earth-Science of Reviews 52, 175–235.

Corbett, D.R., Chanton, J.P., Burnett, W.C., Dillon, K., Rutkowski, C., Fourqurean, J., 1999. Patterns of groundwater discharge into Florida Bay. Limnology and Oceanography 44, 1045–1055.

Elhatip, H., 2003. The use of hydrochemical techniques to estimate the discharge of Ovacik submarine springs on the Mediterranean coast of Turkey. Environmental Geology 43, 714–719.

Elsinger, R.J., Moore, W.S., 1984. ^{226}Ra and ^{228}Ra in the mixing zones of the Pee Dee River-Winyah Bay, Yangtze River and Delaware Bay estuaries. Estuarine, Coastal and Shelf Science 18, 601–613.

Hwang, D.W., Kim, G., Lee, Y.W., Yang, H.S., 2005a. Estimating submarine inputs of groundwater and nutrients to a coastal bay using radium isotopes. Marine Chemistry 96, 61–71.

Hwang, D.W., Lee, Y.W., Kim, G., 2005b. Large submarine groundwater discharge and benthic eutrophication in Bangdu Bay on volcanic Jeju Island, Korea. Limnology and Oceanography 50, 1393–1403.

Johannes, R.E., 1980. The ecological significance of the submarine discharge of groundwater. Marine Ecology Progress Series 3, 365–373.

Jung, H.Y., Cho, K.J., 2003. SOD and inorganic nutrient fluxes from sediment in the downstream of the Nagdong River. Korean Journal of Limnology 36, 322–335.

Kelly, R.P., Moran, S.B., 2002. Seasonal changes in groundwater input to a well-mixed estuary estimated using radium isotopes and implications for coastal nutrient budgets. Limnology and Oceanography 47, 1796–1807.

Kim, D.H., Park, C., 1998. Estimation of nutrients released from sediments of Deukryang Bay. Journal of the Korean Environmental Sciences Society 7, 425–431.

Kim, G., Hwang, D.W., 2002. Tidal pumping of groundwater into the coastal ocean revealed from submarine ^{222}Rn and CH_4 monitoring. Geophysical Research Letters 29. doi:10.1029/2002GL015093.

Kim, H.D., Kim, J.I., Ryu, C.R., 2001a. Study on current and water quality characteristics in Yongil Bay. Journal of Ocean Engineering and Technology 15, 28–37.

Kim, G., Burentt, W.C., Dulaiova, H., Swarsenski, P.W., Moore, W.S., 2001b. Measurement of ^{224}Ra and ^{226}Ra activities in natural waters using a radon-in-air monitor. Environmental Science and Technology 35, 4680–4683.

Kim, G., Lee, K.K., Park, K.S., Hwang, D.W., Yang, H.S., 2003. Large submarine groundwater discharge (SGD) from a volcanic island. Geophysical Research Letters 30. doi:10.1029/2003GL018378.

Kim, G., Ryu, J.W., Yang, H.S., Yun, S.T., 2005. Submarine groundwater discharge (SGD) into the Yellow Sea revealed by ^{228}Ra and ^{226}Ra isotopes: implications for global silicate fluxes. Earth and Planetary Science Letters 237, 156–166.

Kohout, F.A., 1966. Submarine springs. A neglected phenomenon of coastal hydrology. In: Hydrology and Water Resource Development – Symp. C.E.N.T.O, Ankara, pp. 391–413.

Lee, M.K., Lim, D.I., Um, I.K., Shin, E.B., Jung, H.S., 2003. Seasonal variation and spatial distribution of water qualities in Youngil Bay, southeast coast of Korea. Journal of Korean Society of Environmental Engineers 25, 898–908.

Li, L., Barry, D.A., Stagnitti, F., Parlange, J.Y., 1999. Submarine groundwater discharge and associated chemical input to a coastal sea. Water Resource Research 35, 3253–3259.

Michael, H.A., Mulligan, A.E., Harvey, C.F., 2005. Seasonal oscillations in water exchange between aquifer and the coastal ocean. Nature 436, 1145–1148.

Moore, W.S., 1996. Large groundwater inputs to coastal waters revealed by ^{226}Ra enrichment. Nature 380, 612–614.

Moore, W.S., 2003. Sources and fluxes of submarine groundwater discharge delineated by radium isotopes. Biogeochemistry 66, 75–93.

Moore, W.S., Reid, D.F., 1973. Extraction of radium from natural waters using manganese-impregnated acrylic fibers. Journal of Geophysical Research 78, 8880–8886.

Moore, W.S., Arnold, R., 1996. Measurement of ^{223}Ra and ^{224}Ra in coastal waters using a delayed coincidence counter. Journal of Geophysical Research 101, 1321–1329.

Park, B.K., Song, M.Y., 1972. A grain size analysis of bottom sediments of Yeongil Bay, Korea. The Journal of the Oceanological Society of Korea 7, 74–85.

Sarine, M.M., Krishnaswami, S., Somayajulu, B.L.K., Moore, W.S., 1990. Chemistry and uranium, thorium and radium isotopes in the Ganges-Brahmaputra river system: weathering processes and fluxes to the bay of Bengal. Geochimica et Cosmochimica Acta 54, 1387–1396.

Shaban, A., Khawlie, M., Abdallah, C., Faour, G., 2005. Geologic controls of submarine groundwater discharge: application of remote sensing to north Lebanon. Environmental Geology 47, 512–522.

Swarzenski, P.W., Reich, C.D., Spechler, R.M., Kindinger, J.L., Moore, W.S., 2001. Using multiple geochemical tracers to characterize the hydrogeology of the submarine spring off Crescent Beach, Florida. Chemical Geology 179, 187–202.

Taniguchi, M., 2002. Tidal effects on submarine groundwater discharge into the ocean. Geophysical Research Letters 29. doi:10.1029/2002GL014987.

Taniguchi, M., Burnett, W.C., Cable, J.E., Turner, I.V., 2002. Investigation of submarine groundwater discharge. Hydrological Processes 16, 2115–2129.

Wright, S.W., Jeffrey, S.W., Mantoura, R.F.C., Lewellyn, C.A., Bjornland, T., Repeta, D., Welschmeyer, N., 1991. Improved HPLC method for the analysis of chlorophylls and carotenoids

from marine phytoplankton. Marine Ecology Progress Series 77, 183–196.

Yang, D.B., 2003. Land-ocean interactions in the coastal zone. Korea Ocean Research and Development Institute, Korea.

Yang, H.S., Hwang, D.W., Kim, G., 2002. Factors controlling excess radium in the Nakdong River estuary, Korea: submrine groundwater discharge versus desorption from riverine particles. Marine Chemistry 78, 1–8.

Yoon, H.S., Lee, I.C., Ryu, C.R., 2003. Spatial and temporal variation characteristics between water quality and pollutant loads of Yeong-il Bay (I) — seasonal variation of river discharge and inflowing pollutant loads. Journal of the Ocean Engineering and Technology 17, 23–30.

Zektzer, I.S., Ivanov, V.A., Meskheteli, A.V., 1973. The problem of direct groundwater discharge to the sea. Journal of Hydrology 20, 1–36.